Bioresorbable Radiopaque Embolic Microspheres:
An Animal Study To Demonstrate Feasibility And Short Term Data

M. Stein[1], M. Rippy[2], F. Clubb[3], T. Lancon[3], D. Bolikal[4], D. Brandom[5], L. Kabalnova[5], S. Barnhill[5], and J. Zeltinger[5]

1. Columbus Radiology Corporation, Columbus, OH. 2. Rippy Pathology Solutions, Inc., Woodbury, MN. 3. CV Path Lab at Texas A&M University, College Station, TX. 4. Rutgers, The State University of New Jersey, Piscataway, NJ. 5. REVA Medical, Inc., San Diego, CA.

INTRODUCTION

Traditionally, embolic agents have been fluoroscopically invisible, necessitating the use of contrast medium. In addition, bioresorbability has not been a feature of traditional embolic agents. Bioresorbable Radiopaque Embolic Microspheres (or "BREMS") are a unique embolic technology that combines sphere radiopacity with bioresorption and potential drug delivery.

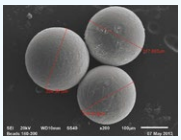

Figure 1. Scanning electron microscope view of BREMS (180-300 microns)

PURPOSE

To provide experimental data on new embolic microspheres, BREMS, with dual properties: radiopacity and bioresorbability. Using conventional angiographic techniques, the visibility, embolization, and biological response to the embolic microspheres were characterized in a mini-swine model.

MATERIALS AND METHODS

Formulations: Polymer formulations were made from polyestercarbonate co-polymers of tyrosine analogs and polyethylene glycol. BREMS (Figure 1) were produced using an emulsion suspension process followed by dry sieving (sizes: 180 – 300, 300 – 400 or 400 – 700 µm diameter).

Microsphere Compressibility: BREMS (280 – 300 µm diameter) were evaluated using a simple cyclic compressive load test to determine their stiffness and resilience.

In Vivo and Post Mortem Evaluations: Each animal protocol followed required guidelines for animal welfare and underwent IACUC approval at American Preclinical Services, LLC (Minneapolis, MN). One Yucatan swine was enrolled for bilateral, renal embolization of the upper and lower poles to evaluate delivery and microsphere visibility acutely (day 0, term). Three Yucatan swine were enrolled for bilateral, renal embolizations of only the lower poles with a scheduled termination at 2 months. BREMS evaluated in vivo were 180 – 300 µm diameter. For embolization, contrast was first injected into the main renal artery to visualize the angiographic anatomy followed by serial saline rinses to flush the contrast (Figure 3A). Next, a 300 mg dose of the BREMS was suspended in saline only and delivered via a 4 French catheter to the lower renal pole (Figure 3B). Kidneys were examined by angiography on 0, 30, and/or 60 days with a Siemens Axiom Artis C-Arm. At each termination, following formalin fixation, the kidneys were evaluated grossly. To detect residual BREMS, after tissue fixation kidneys were examined using high resolution, X-Tek Hawk x-ray and micro-computed tomography (MCT). The biological response was determined using standard light microscopy (hematoxylin and eosin and Gomori's trichrome stains).

RESULTS

Microsphere Compressibility: BREMS were shown to have suitable compressibility (stiffness). The resilience (sphere geometry recovery) of the BREMS is excellent: after 10 cycles of 80% compression, they recovered 80% to 85% of their original size (Figure 2).

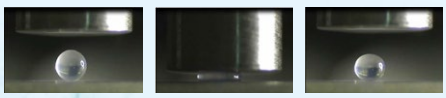

Figure 2. A single BREMS going through a complete compression test.

In Vivo and Post Mortem Evaluations:

Day 0 – Microsphere Visibility and Effectiveness of Embolization: No contrast was used for suspension of BREMS in order to evaluate the visibility of BREMS during delivery. As microspheres exited the catheter, the deposition of BREMS and their depth of penetration and distribution were evident in vivo by fluoroscopy (Figure 3B). Follow-up angiography was performed demonstrating post embolic vascular occlusion. The radiopacity of BREMS allowed excellent procedural control for region-specific, targeted embolization. BREMS indeed acted like contrast agent during embolization.

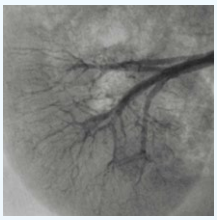

Figure 3A. Day 0: Baseline contrast renal angiography.

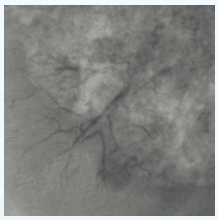

Figure 3B. Day 0: Post-embolization with BREMS; Radiopacity only from embolic agent.

The day 0 post-treatment x-ray (Figure 4A) and MCT (Figure 4B) show densely packed radiopaque microspheres in renal vessels of different sizes.

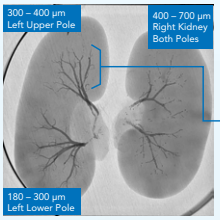

Figure 4A. Day 0 Post-mortem. X-Ray.

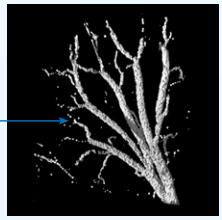

Figure 4B. Day 0 Post-mortem. MCT.

Day 60 – Biological Response / Gross Changes: All 3 animals survived to 60 days without complications. Grossly, compared to an untreated kidney (Figure 5A), all six embolized kidneys showed an obvious reduction in parenchyma, which ranged from 10% to 90%, in the treated caudal pole (example, Figure 5B). All kidneys were trimmed into 3 mm thick sections; no evidence of thrombosis, hemorrhage, or inflammation in the treated or untreated poles was seen (Figure 5C). The remaining parenchyma of the treated caudal pole for each case appeared grossly unaffected with the exception of a distinct, irregularly shaped, subcapsular scar from atrophy. (Figure 5C).

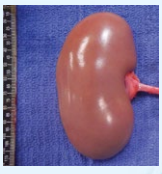

Figure 5A. A normal untreated kidney from an age-matched Yucatan mini-swine.

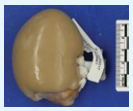

Figure 5B. Day 60: Kidney post embolization showing 90% reduction in parenchyma at the caudal pole.

Figure 5C. Day 60: The same kidney appears grossly normal on cut sagittal section with the exception of the subcapsular scar from atrophy.

Day 60 – Biological Response / Residual BREMS: The radiographs and high resolution MCT identified the residual BREMS at 60 days. In comparison to the MCT (Figure 4B) at day 0 which showed densly packed, individual microspheres, the BREMS at 60 days appeared as fragments and/or a coalescence of the material in the atrophied caudal pole of the kidney (Figures 6A & 6B).

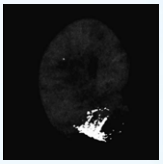

Figure 6A. Day 60: BREMS are localized to only the caudal pole.

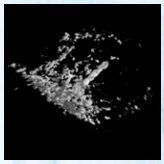

Figure 6B. Day 60: BREMS appear as fragmented material in the treatment region that had atrophied.

Day 60 – Biological Response / Histology: H&E sections showed the presence of residual BREMS material in the remnant of the caudal pole of each kidney. BREMS underwent extravasation through the arterial wall, as seen in multiple vessels, and resulted in engulfment by macrophages in these perivascular locations (Figures 7A & 7B). These areas were largely devoid any other types of inflammatory cells. The remaining renal parenchyma bordering the targeted area of infarction appeared within normal limits and was devoid of any noteworthy inflammatory changes. Occasional microspheres were seen in small numbers of glomeruli of the kidney. The BREMS material appeared amorphous (as evident on Gomori trichrome-stained sections, Figure 7C) and as variably-sized perivascular vacuoles indicating ongoing degradation at 60 days.

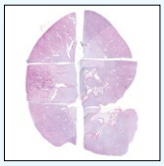

Figure 7A: Day 60: A 3 mm sagittal slice of the same kidney shown above. H&E images were assembled into a montage to show the normal cranial pole and residual caudal pole with subcapsular scar from contracture.

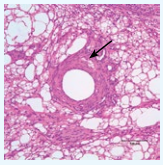

Figure 7B: Day 60: H&E section showing BREMS extravasation occurring through the vessel wall (arrow). The perivascular tissue shows large accumulations of vacuolated macrophages which engulfed the amorphous BREMS.

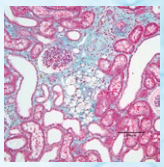

Figure 7C: Day 60: Gomori trichrome-stained sections showing BREMS in vacuolated macrophages amongst glomeruli and tubules.

CONCLUSIONS

The feasibility of controlled embolization was proved without angiographic contrast. The radiopacity of BREMS allowed in vivo visual monitoring of region-specific embolization and their compressibility/recovery facilitated delivery through a 4 French catheter for targeted embolization. Biologically, BREMS were biocompatible with signs of active bioresorption including macrophage phagocytosis. Embolization resulted in well-demarcated areas of ischemia, no significant inflammatory response and preservation of non-embolized tissue. With the ease of use and successful embolization demonstrated, BREMS could now be studied over a time course to characterize the rate of resorption, and ideally, to investigate vascular recanalization.

ACKNOWLEDGEMENTS

The authors express their gratitude to the staff of American Preclinical Services for their interventional expertise, to Texas Heart Institute for their tissue processing for histology, to A. Crotteau (REVA Medical, Inc.) for his assistance with microsphere production, to W. DePolo (REVA Medical, Inc.) and D. Wall (General Atomics) for their SEM imaging and to E. Nesseler and her staff (REVA Medical, Inc.) for performing GPC analyses.